MPI-PhT/94-22
LMU–3/94
April 1994

Light Gluinos and the Parton Structure of the Nucleon *

R. Rückl [a,b] and A. Vogt [a]

[a] Sektion Physik, Universität München, Theresienstraße 37
D–80333 Munich, Germany

[b] Max-Planck-Institut für Physik, Werner-Heisenberg-Institut, Föhringer Ring 6
D–80805 Munich, Germany

Abstract

We study the effects of light gluinos with $m_{\tilde{g}} \lesssim 1$ GeV on the nucleon parton densities and the running of α_S. It is shown that from the available high-statistics DIS data no lower bound on the gluino mass can be derived. Also in the new kinematical region accessible at HERA the influence of such light gluinos on structure functions is found to be very small and difficult to detect. For use in more direct searches involving final state signatures we present a radiative estimate of the gluino distribution in the nucleon.

* Work supported by the German Federal Ministry for Research and Technology under contract No. 05 6MU93P

1 Introduction

The values of the strong coupling constant $\alpha_S(Q)$ as determined from fixed-target deep inelastic lepton-nucleon scattering (DIS) and from hadronic decays of the Z-boson at LEP slightly deviate from the running predicted by QCD [1, 2]. This observation has kindled renewed speculations about the possible existence of a light gluino [3] with a mass of at most a few GeV [4, 5, 6, 7]. The presence of such a light gluino would slow down the decrease of $\alpha_S(Q)$ between the average scale $Q \simeq 5$ GeV of the DIS measurements and the Z-mass and thus improve the overall agreement of experiment with theory [6, 7]. The latest α_S-determinations have reduced the original discrepancy mainly because of a slightly smaller hadronic width of the Z [2]. Within errors, the observed running is now consistent with standard QCD as well as with the hypothesis of a light majorana gluino. Since also other measurement do not convincingly rule out light gluinos [8], this chapter is not yet closed.

If a light gluino exists, it does not only modify the running of $\alpha_S(Q)$, but also the evolution of parton densities and DIS structure functions [9, 10]. It is therefore interesting to investigate the question whether or not one can derive lower bounds on the gluino mass from present or future structure function measurements alone. Such a bound could not be undermined by theoretical uncertainties and would thus put an unavoidable constraint. Following ref. [11] it is reasonable to concentrate on the mass windows $m_{\tilde{g}} \lesssim 1$ GeV and 3 GeV $\lesssim m_{\tilde{g}} \lesssim 5$ GeV. Gluinos in the upper mass range do not significantly change the successful description of fixed-target DIS, direct photon and Drell-Yan lepton pair production obtained by global fits [12, 13] in the framework of the QCD improved parton model. Furthermore, also extrapolations of DIS structure functions to the new kinematical regime accessible at HERA show only little sensitivity to a gluino in this mass range [14]. However, it is a priori not obvious whether these conclusions also apply to the lower mass window $m_{\tilde{g}} < 1$ GeV. Such very light gluinos would carry as much as about 10% of the nucleon momentum already at scales probed in fixed-target DIS. Thus the task remains to clarify whether existing DIS data (including first HERA results at small x [15, 16]) rule out the existence of light gluinos below 1 GeV. If this is not the case, the question arises whether one can expect observable effects later at HERA when more statistics will be accumulated in particular at large x and large Q^2.

Some of these issues have been investigated in a very recent analysis [17] following

the procedure of the CTEQ collaboration [13]. It is concluded that the fixed-target data do not discriminate between the presence and absence of light gluinos. On the other hand, the scaling violations at $x \lesssim 10^{-2}$ are found to be distinctly different in these two cases, whence small-x data from HERA should soon provide decisive tests. This finding, however, contradicts the results of ref. [14] for the common mass $m_{\tilde{g}} = 5$ GeV.

In the present paper, we study the questions raised above within the framework of radiatively generating the parton densities from low-scale valence-like input distributions [18]. This approach is especially well suited for the incorporation of a new particle species with a mass below the input scale $Q_0 \simeq 2$ GeV of conventionally fitted parton distributions [12, 13], since it avoids the introduction of an additional unknown input function. For the gluino, this initial distribution cannot be well determined by a global fit, while our procedure leads to a rather definite prediction. This radiative estimate of the gluino density in the proton is useful for the study of more direct searches using final state signatures [6, 7, 17]. As far as DIS structure functions are concerned, we find no significant effects from gluinos with $m_{\tilde{g}} \lesssim 1$ GeV, neither in the kinematical regime explored so far, nor in the new region accessible to HERA. Thus our analysis does not confirm the low-x results of ref. [17] mentioned above.

The paper is organized as follows: In section 2, we recall the formalism for including a light gluino in the Q^2-evolution of hadronic parton densities [9, 10] and derive the analytical Mellin-n space solution of the modified evolution equations. In section 3, we then explain our phenomenological procedure and present fits to a suitably chosen subset of the available high-statistics DIS measurements. The emerging parton distributions and their implications are discussed in section 4. Finally, in section 5, we summarize our results.

2 Theoretical Framework

In this section we formulate the evolution of parton densities in next-to-leading order (NLO) in the presence of a light majorana gluino. The corresponding standard QCD results can be recovered by simply dropping the gluino-gluon and gluino-quark splitting functions together with the gluino effects in the usual splitting functions. All expressions

will be given in n-moment space defined by the Mellin transformation

$$a^n = \int_0^1 dx\, x^{n-1} a(x) \ . \tag{1}$$

In this representation, the convolutions in evolution equations and structure functions reduce to ordinary products. As a consequence, the equations can be solved analytically. The inverse Mellin transformation back to Bjorken-x space has then to be performed numerically.

The strong coupling constant in NLO can be written in the form

$$\frac{\alpha_S(Q^2)}{4\pi} = \frac{1}{\beta_0 \ln(Q^2/\Lambda^2)} - \frac{\beta_1}{\beta_0^3} \frac{\ln\ln(Q^2/\Lambda^2)}{[\ln(Q^2/\Lambda^2)]^2} \ . \tag{2}$$

The (scheme-independent) coefficients of the β-function are given by

$$\beta_0 = 11 - (2/3)f \ , \quad \beta_1 = 102 - (38/3)f \tag{3}$$

in the standard QCD case, and by

$$\beta_0 = 9 - (2/3)f \ , \quad \beta_1 = 54 - (38/3)f \tag{4}$$

in the presence of a majorana gluino. Here f denotes the number of relevant quark flavours. The QCD scale parameter Λ depends on this number as well as on the renormalization scheme. For the present analysis we employ, as usual, the $\overline{\rm MS}$ scheme. As can be seen from eqs. (3) and (4), a light gluino slows down the running of $\alpha_S(Q^2)$.

Beyond the leading logarithmic approximation parton densities and their evolution depend on the factorization scheme, i.e. on the definition of the coefficient functions C_i entering the moments of the familiar structure functions F_1 and F_2:

$$(\delta_i F_i)^n(Q^2) = \sum_{k=1}^{f} e_k^2 \Big\{ \Big(1 + \frac{\alpha_S(Q^2)}{2\pi} C_{i,q}^n\Big) [q_k^n(Q^2) + \bar{q}_k^n(Q^2)] + \frac{\alpha_S(Q^2)}{2\pi} \frac{1}{f} C_{i,G}^n G^n(Q^2) \Big\} \ , \tag{5}$$

where $\delta_1 = 2$, $\delta_2 = 1/x$. $(\bar{q}_k)\, q_k$ and G denote the (anti-)quark and gluon distributions, respectively, and e_k is the electric charge in units of the electron charge. In contrast to ref. [10], we adopt the $\overline{\rm MS}$ scheme [19]. This allows for a direct comparison of the resulting parton densities with distributions from conventional QCD analyses. Since the gluino coupling to electroweak gauge bosons is $\mathcal{O}(\alpha_S^2)$, the NLO coefficient functions C_i^n are the same with and without a gluino. The explicit expressions in $\overline{\rm MS}$ can be found in ref. [20].

In the $\overline{\rm MS}$ scheme the massive quark flavours and the gluino can be included in the evolution as follows [21]: Below the threshold $Q^2 = m_h^2$ the heavy degree of freedom h is

neglected in the evolution of parton densities as well as in the coefficients (3) and (4) of the β-function. At $Q^2 > m_h^2$ it participates in the evolution and the running of $\alpha_S(Q^2)$ like a massless flavour but with the boundary condition

$$h^n(m_h^2) = 0 \ . \tag{6}$$

This guarantees the continuity of the parton densities at threshold. The $\overline{\rm MS}$ scale parameter $\Lambda^{(f)}$ is changed at $Q^2 = m_h^2$ by the amount necessary to ensure continuity of $\alpha_S(Q^2)$.

In the presence of a gluino the evolution equations read

$$\begin{aligned} \frac{d}{d\ln Q^2} v^n_{\eta,i}(Q^2) &= \frac{\alpha_S(Q^2)}{2\pi}\left(P^{(0)n}_{qq} + \frac{\alpha_S(Q^2)}{2\pi} P^{(1)n}_{\eta}\right) v^n_{\eta,i}(Q^2) \\ \frac{d}{d\ln Q^2} \vec{q}^{\,n}(Q^2) &= \frac{\alpha_S(Q^2)}{2\pi}\left(\hat{P}^{(0)n} + \frac{\alpha_S(Q^2)}{2\pi} \hat{P}^{(1)n}\right) \vec{q}^{\,n}(Q^2) \ . \end{aligned} \tag{7}$$

We have simplified the equations by introducing the usual non-singlet combinations of quark flavours ($i = 1, \ldots, f$),

$$v^n_{-,i} = q^n_i - \bar{q}^n_i \ , \quad v^n_{+,i^2-1} = \sum_{k=1}^{i} (q^n_k + \bar{q}^n_k) - i(q^n_i + \bar{q}^n_i) \ , \tag{8}$$

together with the vector of singlet moments

$$\vec{q}^{\,n} = \begin{pmatrix} \Sigma^n \\ G^n \\ \tilde{g}^n \end{pmatrix} \ , \quad \Sigma^n = \sum_{i=1}^{f} (q^n_i + \bar{q}^n_i) \ , \tag{9}$$

f being again the number of active quark flavours. The moments of the splitting functions are generically denoted by $P^{(0)n}$ and $P^{(1)n}$ in first and second order, respectively. Note that no additional non-singlet combination involving the gluino distribution $\tilde{g}^n(Q^2)$ occurs since we only consider majorana gluinos here.

The splitting functions in eq. (7) can be expressed in terms of the standard QCD quark and gluon splitting functions by a change of colour factors. In lowest order, $P^{(0)n}_{qq}$ is unchanged, while the modified singlet matrix $\hat{P}^{(0)n}$ is given by [9]

$$\hat{P}^{(0)n} = \begin{pmatrix} P^{(0)n}_{qq} & 2f P^{(0)n}_{qG} & 0 \\ P^{(0)n}_{Gq} & P^{(0)n}_{GG} - 1 & \frac{9}{4} P^{(0)n}_{Gq} \\ 0 & 6 P^{(0)n}_{qG} & \frac{9}{4} P^{(0)n}_{qq} \end{pmatrix} \ . \tag{10}$$

Note the absence of quark-gluino splitting in LO and the modification of the gluon-gluon splitting function by the gluino contribution to the gluon self-energy graph. The main

effect of the gluino on the quarks and gluons is a reduction of the gluon density. The second order quantities $P_\eta^{(1)n}$ and $\hat{P}^{(1)n}$ follow from those without a gluino by changing the group factors as described in table 1 of ref. [10][1]. The explicit expressions for integer values of n can be inferred from the appendix of ref. [20] using $P^{(0)n} = -\gamma^{(0)n}/4$ and $P^{(1)n} = -\gamma^{(1)n}/8$. The analytic continuation to complex n, necessary for the Mellin inversion of eq. (1), is explained in ref. [22].

The solution of the non-singlet part of eq. (7) is straightforward. One finds

$$v_{\eta,i}^n(Q^2) = \left\{1 - \frac{\alpha_S(Q^2) - \alpha_S(Q_0^2)}{\pi\beta_0}\left(P_\eta^{(1)n} - \frac{\beta_1}{2\beta_0}P_{qq}^{(0)n}\right)\right\}\left(\frac{\alpha_S(Q^2)}{\alpha_S(Q_0^2)}\right)^{-(2/\beta_0)P_{qq}^{(0)n}} v_{\eta,i}^n(Q_0^2) \ . \tag{11}$$

In the singlet case, the situation is more complicated due to the non-commutativity of the matrices $\hat{P}^{(0)}$ and $\hat{P}^{(1)}$. An implicit solution is given by

$$\begin{aligned}\vec{q}^n(Q^2) \ &= \ \left\{\left[\alpha_S(Q^2)/\alpha_S(Q_0^2)\right]^{-(2/\beta_0)\hat{P}^{(0)n}} + \frac{\alpha_S(Q^2)}{2\pi}\hat{U}^n\left[\alpha_S(Q^2)/\alpha_S(Q_0^2)\right]^{-(2/\beta_0)\hat{P}^{(0)n}}\right. \\ &\left. -\frac{\alpha_S(Q_0^2)}{2\pi}\left[\alpha_S(Q^2)/\alpha_S(Q_0^2)\right]^{-(2/\beta_0)\hat{P}^{(0)n}}\hat{U}^n\right\}\vec{q}^n(Q_0^2) \ ,\end{aligned} \tag{12}$$

where the subleading evolution matrix $\hat{U}$ is fixed by the commutation relation

$$[\hat{U}^n, \hat{P}^{(0)n}] = \frac{\beta_0}{2}\hat{U}^n + \hat{R}^n \ , \quad \hat{R}^n \equiv \hat{P}^{(1)n} - \frac{\beta_1}{2\beta_0}\hat{P}^{(0)n} \ . \tag{13}$$

In order to determine $\hat{U}$, we expand the matrix (10) following ref. [23]:

$$\hat{P}^{(0)n} = \sum_{i=1}^{3} \hat{e}_i^n \lambda_i^n \tag{14}$$

with λ_i^n denoting the eigenvalues of $\hat{P}^{(0)n}$. The arbitrarily normalized eigenvectors $\vec{v}_i$

$$\vec{v}_i = \begin{pmatrix} 2fP_{qG}^{(0)}/(\lambda_i - P_{qq}^{(0)}) \\ 1 \\ 6P_{qG}^{(0)}/(\lambda_i - \frac{9}{4}P_{qq}^{(0)}) \end{pmatrix} \tag{15}$$

build up the projection matrices

$$(\hat{e}_i)_{\alpha\beta} = v_{\alpha i}v_{i\beta}^{-1} \ , \tag{16}$$

[1]There are two misprints in table 1 of ref. [10]: the $C_F N_F$ entries of GL and NS_L should both read $C_\lambda(N_F + N_\lambda)$.

where $v_{\alpha i} \equiv (\vec{v}_i)_\alpha$. Substituting $\hat{U} = \sum_{i,j=1}^{3} \hat{e}_i \hat{U} \hat{e}_j$ and (14) into eq. (13) one readily derives

$$\hat{U} = -\frac{2}{\beta_0} \sum_{i=1}^{3} \hat{e}_i \hat{R} \hat{e}_i + \sum_{\substack{i,j=1 \\ i \neq j}}^{3} \frac{\hat{e}_i \hat{R} \hat{e}_j}{\lambda_j - \lambda_i - \beta_0/2} \ . \tag{17}$$

For simplicity of writing, we have suppressed the superscript n in (15–17). Eqs. (12) and (17) then yield the explicit singlet solution

$$\begin{aligned} \vec{q}^{\,n}(Q^2) \ = \ & \left\{ \sum_{i=1}^{3} \left(\frac{\alpha_S(Q^2)}{\alpha_S(Q_0^2)} \right)^{-2\lambda_i^n/\beta_0} \left[\hat{e}_i^n + \frac{\alpha_S(Q_0^2) - \alpha_S(Q^2)}{2\pi} \frac{2}{\beta_0} \hat{e}_i^n \hat{R}^n \hat{e}_i^n \right. \right. \\ & \left. \left. - \sum_{j \neq i} \left(\frac{\alpha_S(Q_0^2)}{2\pi} - \frac{\alpha_S(Q^2)}{2\pi} \left(\frac{\alpha_S(Q^2)}{\alpha_S(Q_0^2)} \right)^{-2(\lambda_j^n - \lambda_i^n)/\beta_0} \right) \frac{\hat{e}_i^n \hat{R}^n \hat{e}_j^n}{\lambda_j^n - \lambda_i^n - \beta_0/2} \right] \right\} \vec{q}^{\,n}(Q_0^2) \ . \end{aligned} \tag{18}$$

Finally, the individual quark distributions can be obtained from the singlet and non-singlet moments (11) and (18) using the relation

$$q_i^n(Q^2) + \bar{q}_i^n(Q^2) = \frac{1}{f} \Sigma^n(Q^2) - \frac{1}{i} v_{+,i^2-1}^n(Q^2) + \sum_{k=i+1}^{f} \frac{1}{k(k-1)} v_{+,k^2-1}^n(Q^2) \ . \tag{19}$$

3 Phenomenological Analysis

We begin with the question whether or not a very light gluino is consistent with the high-statistics fixed-target DIS measurements. To find the answer it is not necessary to carry out a complete global fit to all data available. Instead we follow ref. [18] and proceed in two steps. First, we study the valence quark region and the strong coupling constant. Using the result as an input we then investigate the more interesting regime at smaller x where the gluon and sea distributions play an important role. Only this second part of the analysis requires new fits to data.

For the valence quark description of F_2 and xF_3 in standard QCD we adopt the NLO proton distributions and the QCD scale parameter from the global fit KMRS(B$_-$) [24][2]. At the reference scale $Q_0^2 = 4$ GeV^2, they are given by

$$\begin{aligned} x(u_v + d_v)(x, Q_0^2) \ &= \ 0.385\, x^{0.27} (1 + 9.9\sqrt{x} + 17.7x)(1-x)^{3.93} \\ x d_v(x, Q_0^2) \ &= \ 1.50\, x^{0.61} (1 + 1.08\sqrt{x})(1-x)^{4.68} \end{aligned} \tag{20}$$

[2]In refs. [24] and [25] a slightly different NLO relation between α_S and Λ has been used. We have transformed their results to the convention (2) employed here, resulting in a 10 MeV increase of $\Lambda^{(4)}$.

and $\Lambda^{(4)} = 200$ MeV. More recent fits exist, the differences in the valence quarks being, however, marginal and completely immaterial for the present purpose. Also the value of $\Lambda^{(4)}$ is consistent with more recent determinations, for example from newer CCFR data giving $\Lambda^{(4)} = (220 \pm 50)$ MeV [25][2]. With a gluino in the mass range $m_{\tilde{g}} < Q_0$ included it is still possible to reproduce $xF_3(x, Q^2)$ and the valence contribution to $F_2(x, Q^2)$ in the measured range, 5 GeV$^2 \lesssim Q^2 \lesssim 300$ GeV^2 and $0.01 \lesssim x \lesssim 0.7$, within less than 0.5 % by a slight modification of the valence quark input and a suitable choice of $\Lambda_{\tilde{g}}^{(4)}$. Hence no new valence fit to data is necessary. Optimization of this agreement leads to

$$\begin{aligned} x(u_v + d_v)(x, Q_0^2)_{\tilde{g}} &= 0.388\, x^{0.27}(1 + 9.9\sqrt{x} + 17.6x)(1 - x)^{3.975} \\ x d_v(x, Q_0^2)_{\tilde{g}} &= 1.51\, x^{0.61}(1 + 1.09\sqrt{x})(1 - x)^{4.74} \end{aligned} \tag{21}$$

together with $\Lambda_{\tilde{g}}^{(4)} = 30$ MeV.

The strong coupling constants $\alpha_S(Q)$ in the two scenarios (20) and (21) coincide at $Q^2 = 12$ GeV^2. The continuity of α_S at the heavy quark thresholds $Q^2 = m_h^2$ $(h = c, b)$ then implies for the NLO scale parameters $\Lambda^{(f)}$ in the $\overline{\rm MS}$ scheme:

$$\begin{aligned} \Lambda^{(3,4,5)} &= 248, 200, 131 \text{ MeV} \\ \Lambda_{\tilde{g}}^{(3,4,5)} &= 56.5, 30, 10.6 \text{ MeV} \ , \end{aligned} \tag{22}$$

where $m_c = 1.5$ GeV, $m_b = 4.5$ GeV and $m_{\tilde{g}} < m_c$ has been used. Obviously, these values of $\Lambda_{\tilde{g}}^{(f)}$ are independent of the gluino mass, but apply only above the gluino threshold $Q = m_{\tilde{g}}$. The gluino mass dependent values of $\Lambda_{\tilde{g}}^{(3)}$ relevant below the gluino threshold will be given later. Using eq. (22) we find $\alpha_S(M_Z) = 0.128\ (0.109)$ with (without) the gluino. The result in brackets agrees with the recent CCFR value, $\alpha_S(M_Z) = 0.111 \pm 0.005$ [25] obtained from a standard QCD analysis. A similar uncertainty in $\alpha_S(M_Z)$ is expected for the gluino case. The existence of a light gluino would, however, not only modify the DIS results on $\alpha_S(Q)$ and the extrapolation to $Q = M_Z$ but also change the direct LEP determinations of $\alpha_S(M_Z)$ due to contributions to virtual and real radiative corrections [7]. With (without) a light gluino one obtains [7, 2] $\alpha_S(M_Z) = 0.132\ (0.120) \pm 0.006$ from hadronic event shapes and $\alpha_S(M_Z) = 0.124\ (0.122) \pm 0.009$ from the hadronic width Γ_h of the Z^0. Note that the original results of ref. [7] have been updated with respect to the latest value of Γ_h. Cleary, within present uncertainties, both scenarios give a consistent picture.

We now turn to the more interesting part of the analysis dealing with the gluon and sea densities. For this, we adopt the radiative approach developed in refs. [22, 18, 26, 27].

This approach provides a unified description of hadronic and photonic parton distributions which agrees with experiment, and which predicted the steep rise of the structure function F_2 at small x discovered recently at HERA [15, 16]. The charactistic features of this framework are a very low scale $(\mu/\Lambda^{(3)})^2 \simeq 5 \div 6$ at which the Altarelli-Parisi evolution is started and valence-like input densities. For light gluinos with $m_{\tilde{g}} > \mu$, this procedure has the advantage that the gluino can approximately be treated like a massive quark with the boundary condition (6). It is generated similarly to the strange sea discussed below. In this way one can avoid the introduction of a gluino input distribution except for almost massless gluinos with $m_{\tilde{g}} < \mu$. For the gluon and sea quark inputs we use [18]

$$\begin{aligned} xG(x,\mu^2) &= Ax^{\alpha}(1-x)^{\beta} \\ x\bar{u}(x,\mu^2) &= x\bar{d}(x,\mu^2) = A'x^{\alpha'}(1-x)^{\beta'} \\ xs(x,\mu^2) &= x\bar{s}(x,\mu^2) = 0 \ . \end{aligned} \tag{23}$$

The vanishing of the strange sea at μ^2 leads to SU(3) breaking in the sea in accordance with experimental results from opposite-sign dimuon events in neutrino-nucleon scattering [28]. The value of μ is fixed by the momentum fraction $<x>_v (\mu^2)$ carried by the valence quarks. For the standard QCD case we take $\mu^2 = 0.3$ GeV^2 corresponding to $<x>_v \simeq 0.6$ [18]. Keeping this fraction also in the presence of a gluino, the scale μ decreases with the gluino mass due to the slower evolution at low Q^2. This correlation is shown in table 1 for typical gluino masses. In order to illustrate the sensitivity of the outcome of the subsequent fits to the exact value of μ we also give results for $\mu^2 = 0.36$ GeV^2, that is, for a 10% increase of μ.

The input parameters appearing in (23) are fitted to the available high-statistics data on F_2^{ed} and $F_2^{\mu d}$ from SLAC [29], BCDMS [30][3] and NMC [32] in the region of good sensitivity, i.e. at $x < 0.3$. Statistical and systematical errors are added in quadrature. As in ref. [12] the BCDMS data is normalized down by 2% relative to the SLAC results. In order to suppress possible higher twist effects we restrict our fits to measurements at $Q^2 > 5$ GeV^2. An additional cut on the invariant mass W of the hadronic final state is not neccessary in view of the low x-values involved. In total, we are left with 147 data points. Additional high precision data on $F_2^{\nu N}$, F_2^p and the ratio F_2^n/F_2^p mainly influence the flavour decomposition, and are unimportant for the gluino issue. Moreover, by using the valence distributions from ref. [24] the main features of these measurements are incorporated. Likewise, data on Drell-Yan lepton pair production mainly constrain

[3]We take the BCDMS data as used in [31], i.e. with a shift of the central values due to the main systematic error. However, in the x-region considered here the effect is not essential.

the shape of the sea quark densities at large x where they are small and not relevant for the present study. On the other hand, data on direct photon production in proton-proton collisions [33] may be relevant, since this process directly probes the gluon distribution which is most affected by light gluinos. However, unlike in the case of DIS and the Drell-Yan process, the hard photon production cross sections in NLO do get modified in the presence of gluinos. These modifications have not yet been calculated. Hence, we disregard the direct photon data in the fits for theoretical consistency but take them into account approximately as discussed below.

$m_{\tilde{g}}$	$\Lambda^{(3)}$/MeV	μ^2/GeV^2	$<x>_v\ (\mu^2)$	α'	β'	A'	χ^2
0.4	118	0.09	0.617	0.490	8.03	0.138	140
0.7	148	0.125	0.618	0.519	8.02	0.134	139
1.0	168	0.155	0.615	0.514	8.03	0.131	137
1.3	184	0.18	0.615	0.525	8.06	0.130	137
no $\tilde{g}$	248	0.30	0.614	0.529	7.93	0.127	134
0.4	118	0.12	0.572	0.362	7.66	0.134	134
0.7	148	0.155	0.578	0.371	7.63	0.130	134
1.0	168	0.19	0.576	0.364	7.59	0.129	133
1.3	184	0.22	0.575	0.364	7.56	0.128	132
no $\tilde{g}$	248	0.36	0.574	0.367	7.44	0.125	130

Table 1: Fits of DIS structure functions to experimental data on F_2^d at $x < 0.3$ and $Q^2 > 5$ GeV^2 (147 data points) in standard QCD (no $\tilde{g}$) and including a light gluino. The input distributions are given in eq. (23) and specified further in the text.

Since the gluon normalization A is fixed by the momentum sum rule, we have five free parameters describing the input distributions (23). These are fitted to the data selected above in the standard QCD case and for several gluino masses $m_{\tilde{g}}$ between 0.4 GeV and 1.3 GeV. The results of the fits are given in table 1. The outcome is almost insensitive to variations of the two shape variables of the gluon density in the range of values favoured by direct photon measurements [33, 34]. For this reason, we simply take

$$\alpha = 2.0\ (1.5)\ , \quad \beta = 4.0 \tag{24}$$

in the fits summarized in the upper (lower) part of the table. Also the sea quark shape parameters α' and β' are only slightly affected by the inclusion of a light gluino. However, the overall normalization A' shows a small but significant rise with decreasing gluino mass. This is exactly what one expects physically since the gluon density, and hence the

evolution of quark-antiquark pairs, is somewhat diminished due to gluino radiation. The quality of the above fits is as good as the one of the recent MRS global analysis [12], if one compares the description of the data used in both fits. As can be seen from the χ^2 values in the last row of table 1 there is no evidence from the fits in favour or against gluinos with masses below 1 GeV. This conclusion agrees with ref. [17].

4 Resulting Parton Distributions

Using the results from the fits outlined in the previous section, we now discuss the parton densities of the nucleon and the structure function F_2^p. This will also enable us to answer the second question raised in the introduction concerning the potential of future DIS measurements at HERA in testing the existence of a very light gluino. As reference cases for comparison we focus on the standard QCD fit with $\mu^2 = 0.30$ GeV^2 and the gluino scenario with $m_{\tilde{g}} = 0.7$ GeV and $\mu^2 = 0.125$ GeV^2.

It is instructive to consider briefly the fractions $<x>_f = \int_0^1 dx\, x f(x, Q^2)$ of the nucleon momentum carried by quarks, gluons and gluinos. Their Q^2-evolution is shown in fig. 1. As the main effect, the average gluon momentum is lowered by gluino radiation. This reduction is fed back to the quarks at large Q^2. Below threshold, at $Q^2 \lesssim m_{\tilde{g}}^2$, the change of the quark and gluon momentum fractions reflects the slower running of $\alpha_S(Q^2)$ in the presence of a gluino. Asymptotically, the gluino momentum reaches about 10% of the proton momentum. Moreover, one can see that already at $Q^2 \simeq 10$ GeV^2 the gluino component gives a non-negligible contribution to the momentum sum rule.

Figs. 2 and 3 exhibit the sea quark distributions $x\bar{u} = x\bar{d}$ and the gluon density xG at $Q^2 = 10$ GeV^2. While the inclusion of the gluino has virtually no effect on the sea quarks, the gluon distribution is reduced by about 15% over the range $x \gtrsim 0.05$. This shrinkage is, however, not expected to lead to phenomenological problems, most notably, in direct photon production, given the present theoretical and experimental uncertainties and taking into account the partial compensation by the larger value of $\alpha_S(Q^2)$ at high Q^2.

The predictions in the small-x region and the Q^2-evolution of $x\bar{u}$ and xG are depicted in figs. 4 and 5. Also here, the gluino effect on the sea quark density can be neglegted for all practical purposes. Furthermore, the depletion of the gluon distribution shown in

fig. 3 for large x disappears as x decreases. All effects depend only weakly on Q^2. In particular, in the region of x and Q^2 currently under investigation at HERA, it appears impossible to uncover a light gluino in the structure functions. This conclusion is further corroborated in fig. 6, where F_2^p is displayed in this kinematical region together with first HERA data [15, 16]. The tiny down-shifts of F_2^p are mainly due to a smaller charm contribution[4] which in turn is a consequence of the lower gluon density. The standard QCD results with $\mu^2 = 0.3$ GeV^2 are practically identical to the q pre-HERA predictions of refs. [18]. The uncertainty in these predictions is illustrated by the expectations for $\mu^2 = 0.36$ GeV^2.

The above findings differ from the results obtained in ref. [17]. While, according to this paper, at $Q^2 = 10$ GeV^2 the quark and gluon distributions are only affected at the 10% level, at $Q^2 = 100$ GeV^2 and $10^{-4} \lesssim x \lesssim 10^{-3}$ the presence of a light gluino gives rise to an increase of xu and xG by about 50%. Moreover, this strong evolution is roughly independent of the gluino mass for $m_{\tilde{g}} \lesssim 5$ GeV. This disagrees also with ref. [14], where a gluino of 5 GeV is shown to change F_2^p by at most a few per cent.

Turning to the Q^2-evolution of structure functions at large x, in fig. 7 we illustrate the changes in F_2^p in the region $Q^2/x < s \simeq 10^5$ GeV^2 which will be probed at HERA. The deviations from the standard QCD evolution are somewhat bigger than the effects found in ref. [14] for $m_{\tilde{g}} = 5$ GeV. This is expected because of the lower gluino mass considered here. However, also for such light gluinos the deviations do not exceed a few per cent and will therefore be very hard to detect [36], in contrast to the expectation in ref. [7] based on the enhancemant of α_S at high scales. This conclusion suggests to return once more to the gluino content in the nucleon considered at the beginning of this section which may play a role in more direct searches at *ep*- and hadron colliders.

Fig. 8 shows distributions in x and the evolution of the gluino component together with the strange sea also generated radiatively from a vanishing input. The threshold dependence is illustrated for the gluino by considering three different masses $m_{\tilde{g}} = 0.4$, 0.7 and 1.0 GeV. At large x, $\tilde{g}(x, Q^2)$ is about three times bigger than $s(x, Q^2)$ and, incidentally, rather similar to $\bar{u}(x, Q^2)$. The ratio $\tilde{g}/s$ rises with decreasing x, reaching a value around five at $x \simeq 10^{-4}$ in accordance with the expectation from the differences in the colour factors of the relevant splitting functions in eq. (10). The relative abun-

[4] Above threshold the charm quark is treated as a massless flavour. Using instead the complete photon-gluon fusion cross section for the charm contribution results in a decrease of F_2^p by $5 \div 10\,\%$ at small x. For a detailed discussion see [35].

dance of gluinos depends only weakly on Q^2 except close to the threshold. Comparing these predictions with the gluon and gluino distributions given in ref. [17] we find rough agreement at $Q^2 = 10$ GeV^2. However, at $Q^2 = 100$ GeV^2 and small x a gluino with $m_{\tilde{g}} \approx 0$ is predicted to be about three times as abundant as what we find. Moreover, it dominates the corresponding up-quark density by almost a factor of nine in contrast to the expectation from eq. (10). We have checked that our evolution program reproduces the results of ref. [14] if the same input is used. Therefore, we believe that fig. 8 represents a reasonable estimate of the gluino content of the proton, if a light gluino exists.

5 Summary

We have investigated the effects of a very light gluino with $m_{\tilde{g}} \lesssim 1$ GeV on the quark and gluon distributions of the nucleon and the DIS structure functions. The whole range in Bjorken-x and Q^2 which is being probed in fixed-target experiments and at HERA has been taken into consideration. We have adopted the framework described in refs. [22, 18] in which the parton densities are generated radiatively from valence-like distributions at a very low input scale. This procedure leads to rather definite predictions at small x which are in agreement with first HERA results [15, 16]. Moreover, in the present application it has the advantage that the light gluino can be included in the Q^2-evolution similarly as a massive quark, i.e. without introducing a perturbatively uncalculable and phenomenologically rather unconstrained gluino input function.

Using $\Lambda^{(f)}_{\overline{MS}}$ as determined from a valence quark analysis of F_2 and xF_3 in the presence of a light gluino, the valence-like input distributions have been fitted to the relevant high-statistics data on F_2^d. Globally, we find that the gluino carries about $5 \div 10\,\%$ of the nucleon momentum. On the other hand, the effects on the quark and gluon distributions at $x \lesssim 10^{-2}$ are completely negligible, even after evolution over a few orders of magnitude in Q^2. The fits to fixed-target data including a light gluino are almost as good as the standard QCD fits. Moreover, we have shown that the structure function F_2^p is practically insensitive to light gluinos also in the new kinematical region covered by HERA. We thus conclude that measurements of DIS structure functions are not able to discriminate between the presence and absence of light gluinos.

Then, in order to test the light-gluino hypothesis one has to study final state signatures

such as jet rates and and displaced vertices. In $\bar{p}p$, pp and ep collisions, this involves the gluino density in the proton. We have presented a radiative estimate for this component assuming that the gluino distribution vanishes at the threshold $Q^2 = m_{\tilde{g}}^2$. Far from threshold the gluino density is predicted to be about three to five times higher than the strange quark density.

References

[1] S. Bethke, Univ. Heidelberg preprint HD–PY–92–13, Review talk at the 26th Int. Conf. on High Energy Physics, Dallas 1992

[2] S. Bethke, Univ. Heidelberg preprint HD–PY–93–07, Lectures at the Scottish Summer School in Physics, St. Andrews, Scotland 1993

[3] G.R. Farrar and P. Fayet, Phys. Lett. B76 (1978) 575

[4] I. Antoniadis, J. Ellis and D.V. Nanopoulos, Phys. Lett. B262 (1991) 109

[5] L. Clavelli, Phys. Rev. D46 (1992) 2112; L. Clavelli, P.W. Coulter and K. Yuan, Phys. Rev. D47 (1993) 1973

[6] M. Jezabek and J.H. Kühn, Phys. Lett. B301 (1993) 121

[7] J. Ellis, D.V. Nanopoulos and D.A. Ross, Phys. Lett. B305 (1993) 375

[8] Particle Data Group, K. Hikasa et al., Phys. Rev. D45 (1993) No. 11, II.34, IX.5

[9] B.A. Campbell, J. Ellis and S. Rudaz, Nucl. Phys. B198 (1982) 1

[10] I. Antoniadis, C. Kounnas and R. Lacaze, Nucl. Phys. B211 (1983) 216

[11] UA1 Coll., C. Albajar et al., Phys. Lett. B198 (1987) 261

[12] A.D. Martin, R.G. Roberts and W.J. Stirling, Phys. Rev. D47 (1993) 867; Phys. Lett. B306 (1993) 147

[13] CTEQ Coll., J. Botts et al., Phys. Lett. B304 (1993) 159

[14] R.G. Roberts and W.J. Stirling, Phys. Lett. B313 (1993) 453

[15] ZEUS Coll., M. Derrick et al., Phys. Lett. B316 (1993) 416

[16] H1 Coll., I. Abt et al., Nucl. Phys. B407 (1993) 515

[17] J. Blümlein and J. Botts, Phys. Lett. B325 (1994) 190

[18] M. Glück, E. Reya and A.Vogt, Z. Phys. C53 (1992) 127; Phys. Lett. B306 (1993) 391

[19] W.A. Bardeen et al., Phys. Rev. D18 (1978) 3998

[20] E.G. Floratos, C. Kounnas and R. Lacaze, Nucl. Phys. B192 (1981) 417

[21] J.C. Collins, W.-K. Tung, Nucl. Phys. B278 (1986) 934

[22] M. Glück, E. Reya and A.Vogt, Z. Phys. C48 (1990) 471

[23] W. Furmanski and R. Petronzio, Z. Phys. C11 (1982) 293

[24] J. Kwiecinski et al., Phys. Rev. D42 (1990) 3645

[25] CCFR Coll., P.Z. Quintas et al., Phys. Rev. Lett. 71 (1993) 1307

[26] M. Glück, E. Reya and A.Vogt, Z. Phys. C53 (1992) 651

[27] M. Glück, E. Reya and A.Vogt, Phys. Rev. D46 (1992) 1973

[28] CCFR Coll., S.A. Rabinowitz et al., Phys. Rev. Lett. 70 (1993) 134

[29] L.W. Whitlow, Ph.D. Thesis, Stanford University, 1990, SLAC-Report-357 (1990)

[30] BCDMS Coll., A.C. Benvenuti et al., Phys. Lett. B237 (1990) 592

[31] A. Milsztain and M. Virchaux, Phys. Lett. B274 (1992) 221

[32] NMC Coll., P. Amaudruz et al., Phys. Lett. B295 (1992) 159

[33] M. Bonesini et al., WA70 Coll., Z. Phys. C38 (1988) 371

[34] P. Aurenche et al., Phys. Rev. D39 (1989) 3275

[35] M. Glück, E. Reya and M. Stratmann, Univ. Dortmund preprint DO–TH 93/20, Nucl. Phys. B, to appear

[36] J. Blümlein et al., Z. Phys. C45 (1990) 501

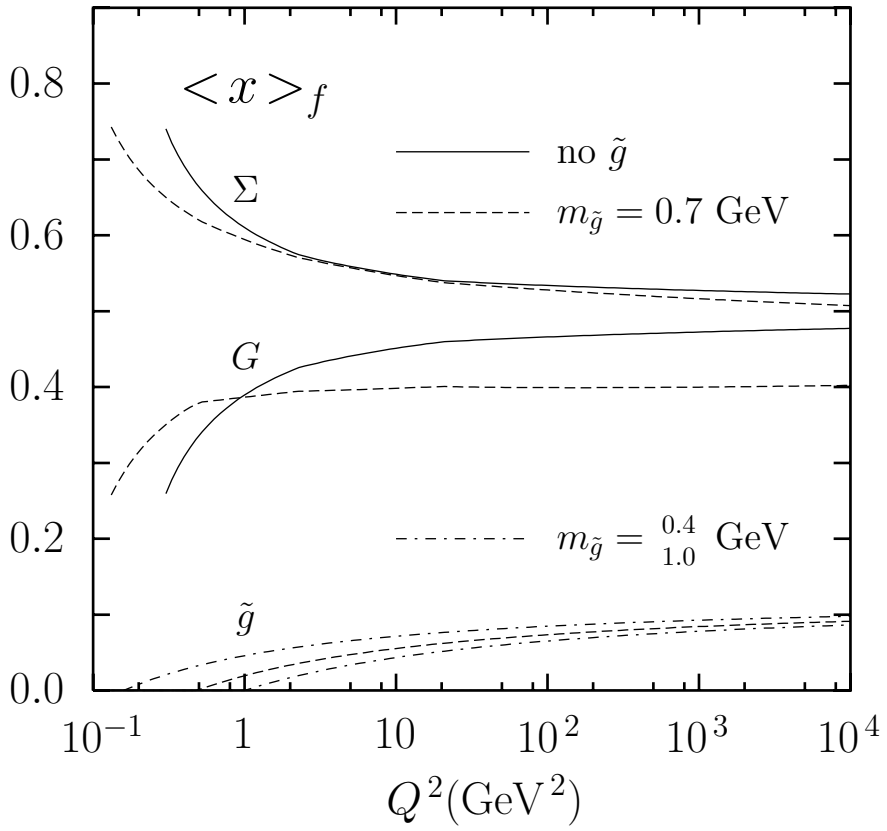

Figure 1: The NLO Q^2-evolution of the momentum fractions $< x >_f$ carried by quarks and gluons in standard QCD and including a light gluino with $m_{\tilde{g}} = 0.7$ GeV. The gluino momentum fraction is given for varying gluino masses.

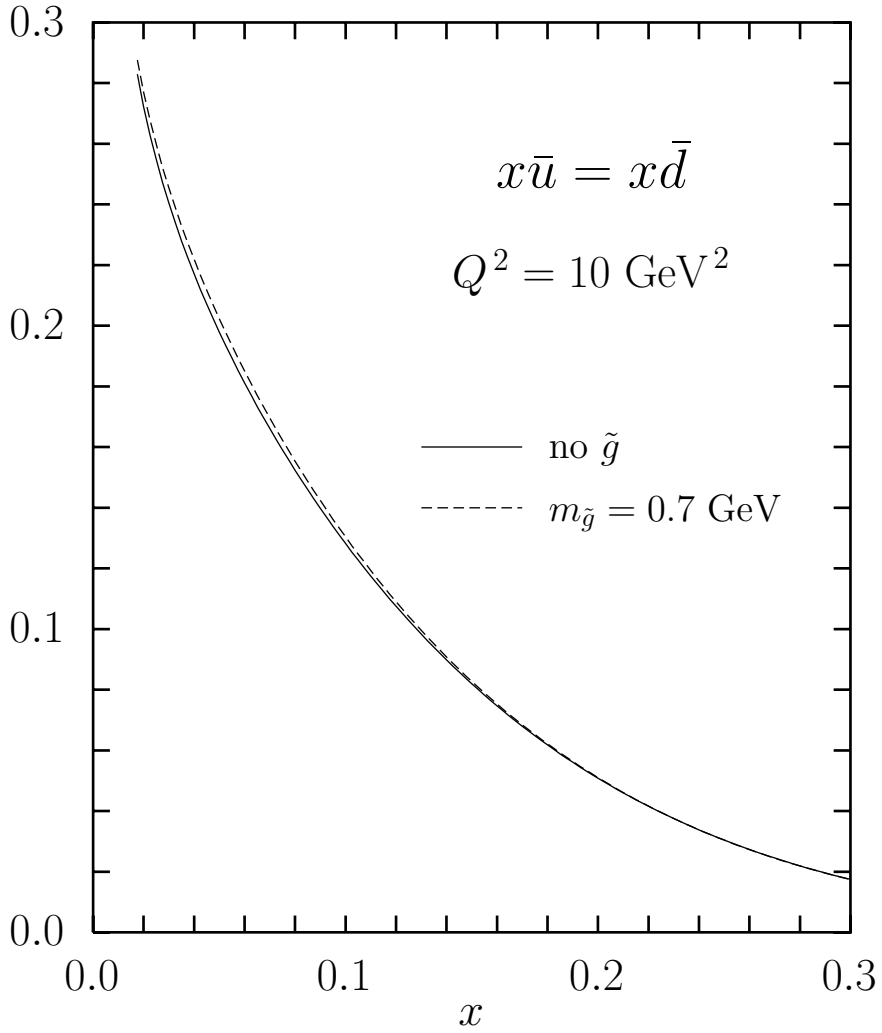

Figure 2: NLO sea quark distribution with and without a light gluino in the x-region probed by fixed-target DIS.

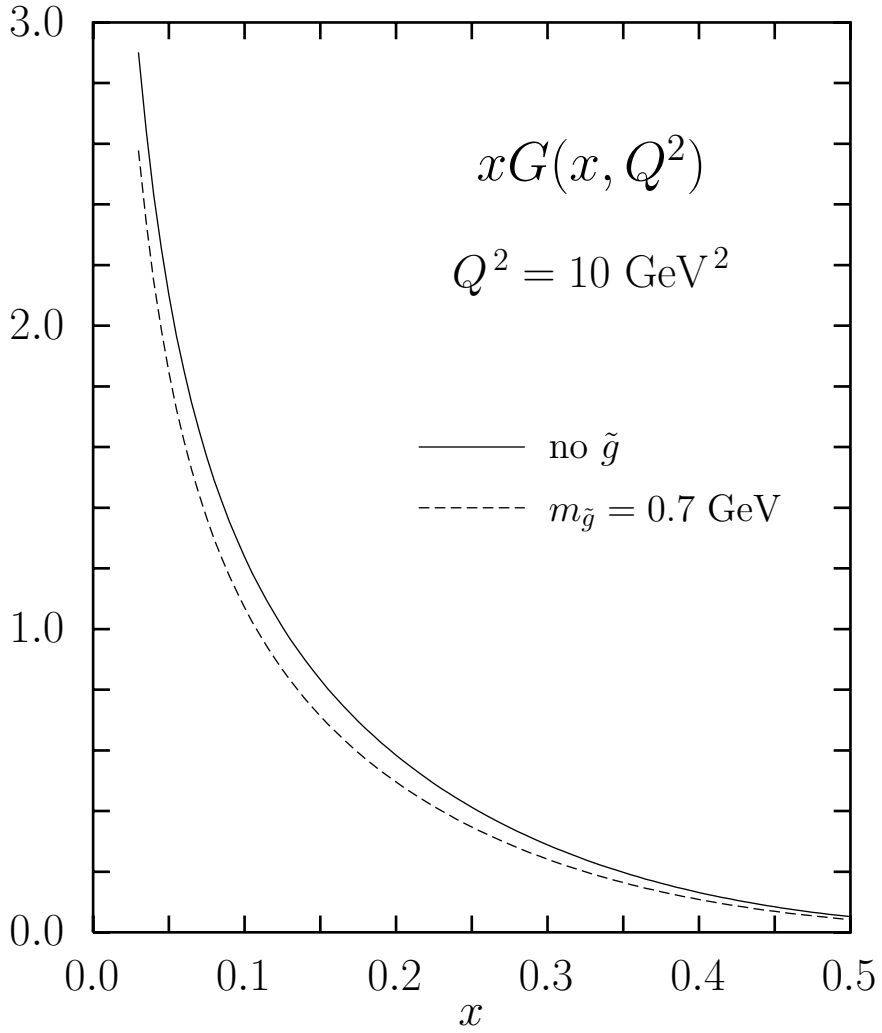

Figure 3: The NLO gluon distribution with and without a light gluino in the x-range probed by fixed-target DIS.

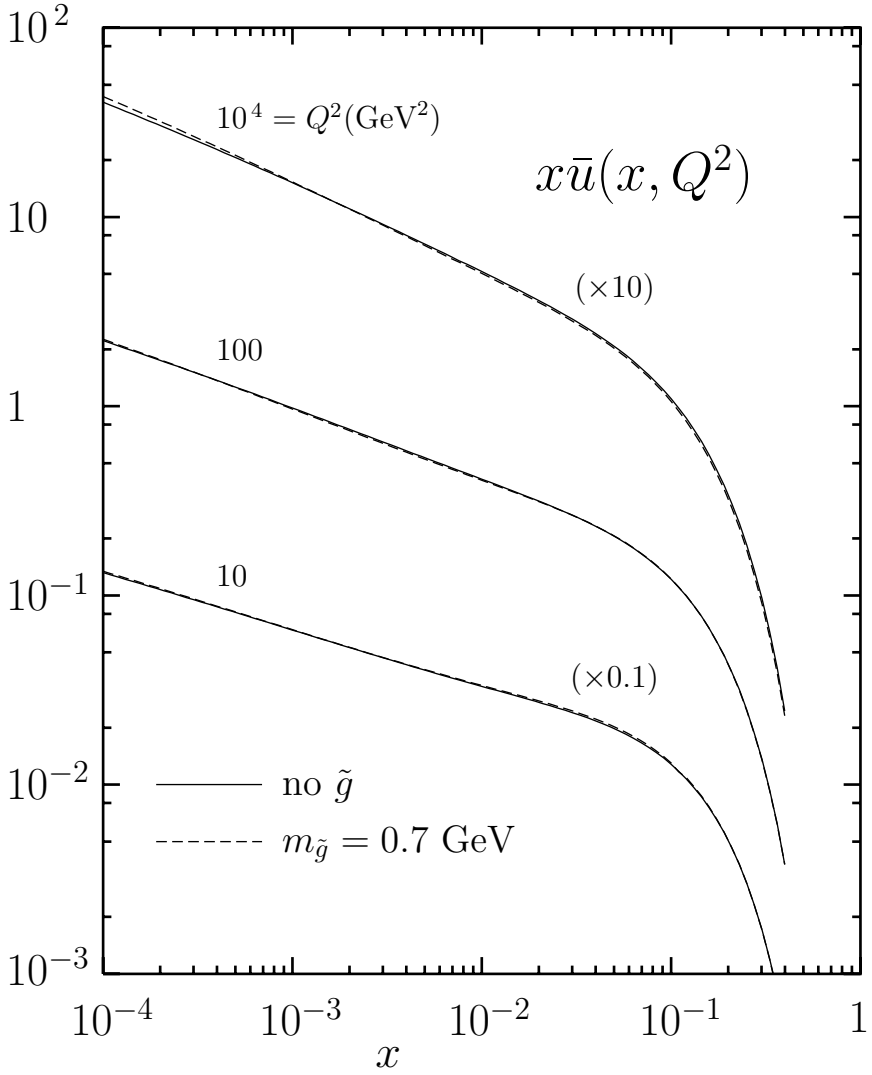

Figure 4: The small-x behaviour of the sea quark density $x\bar{u} = x\bar{d}$ and its evolution in Q^2. Compared are predictions with and without a light gluino.

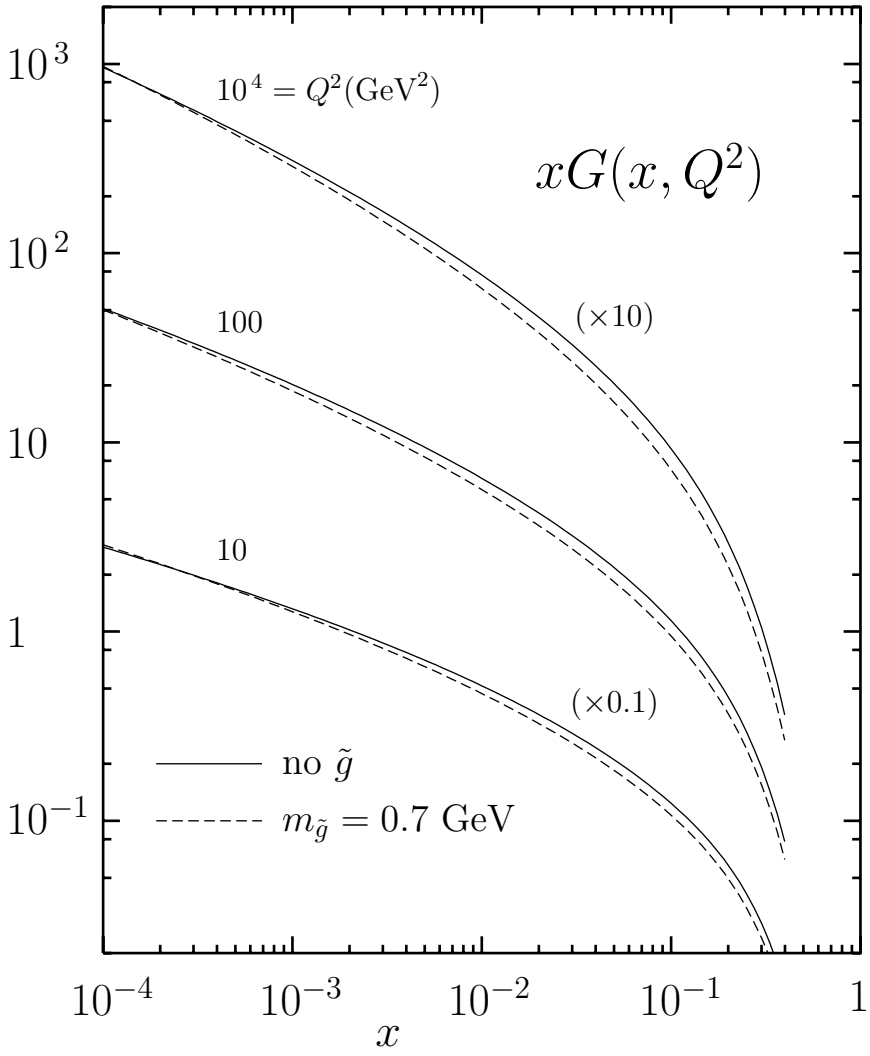

Figure 5: Same as fig. 4, but for the gluon distribution.

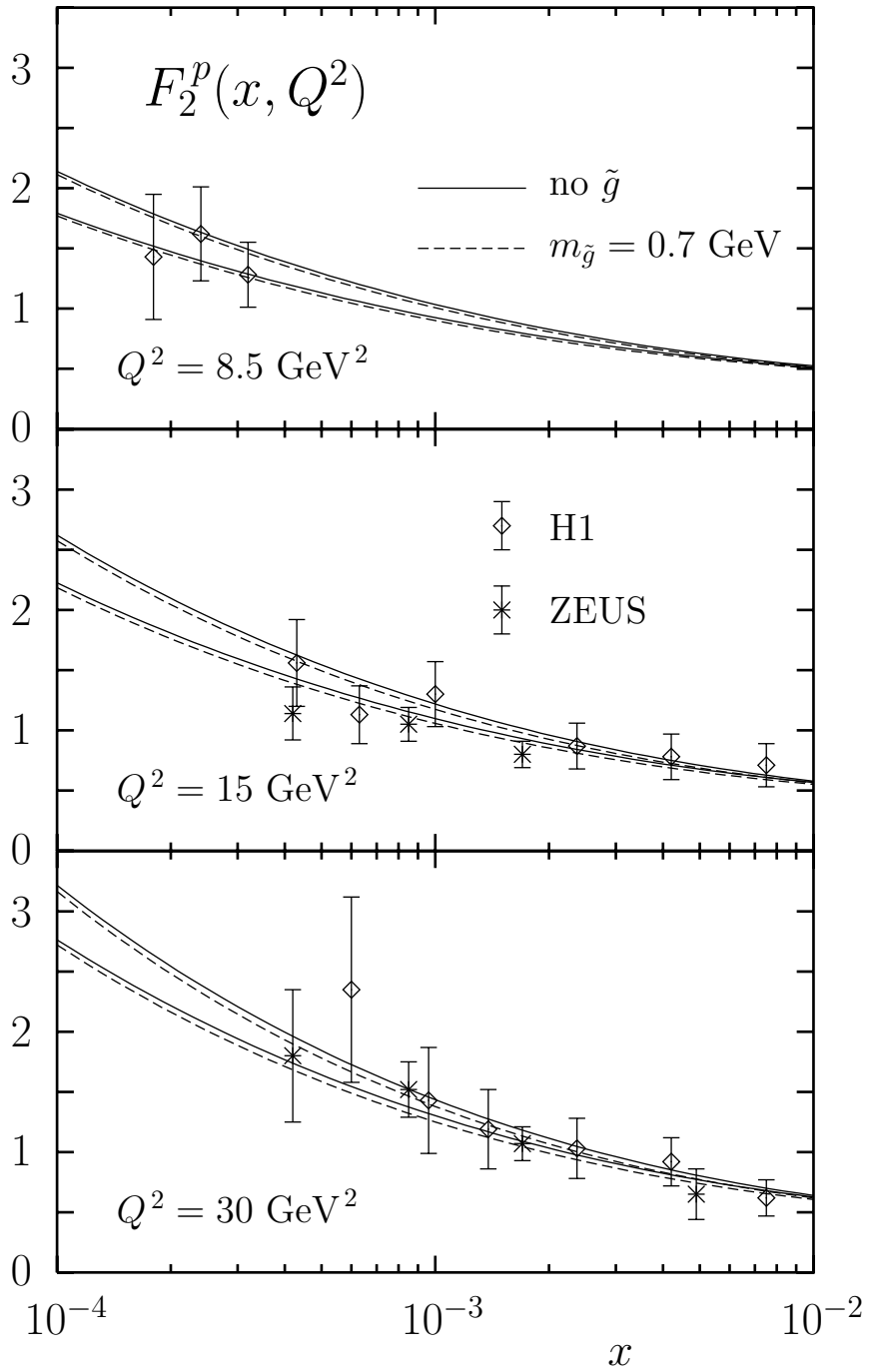

Figure 6: NLO predictions for the proton structure function F_2^p at small x in comparison to first HERA data from the ZEUS [15] and H1 [16] collaborations. The solid curves represent the standard QCD results for the input scales $\mu^2 = 0.3\,\mathrm{GeV}^2$ (upper) and $\mu^2 = 0.36\,\mathrm{GeV}^2$ (lower). The dashed curves show the corresponding predictions with a light gluino included.

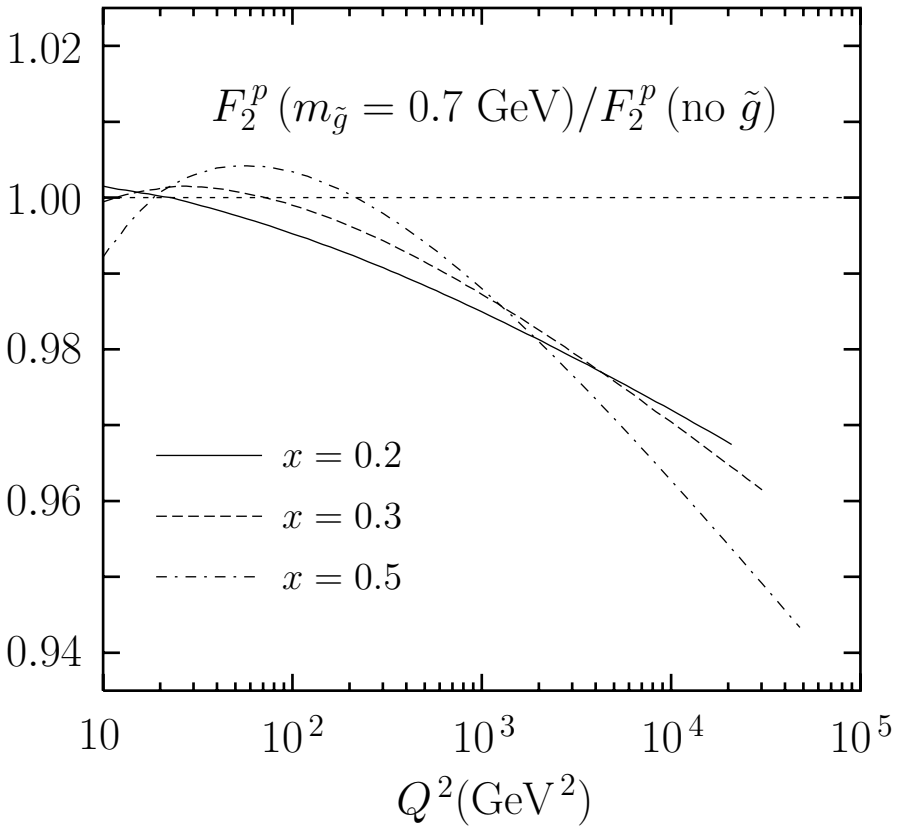

Figure 7: The ratio of the structure functions F_2^p with and without a light gluino as extrapolated from our fits into the large-x, large-Q^2 region accessible at HERA.

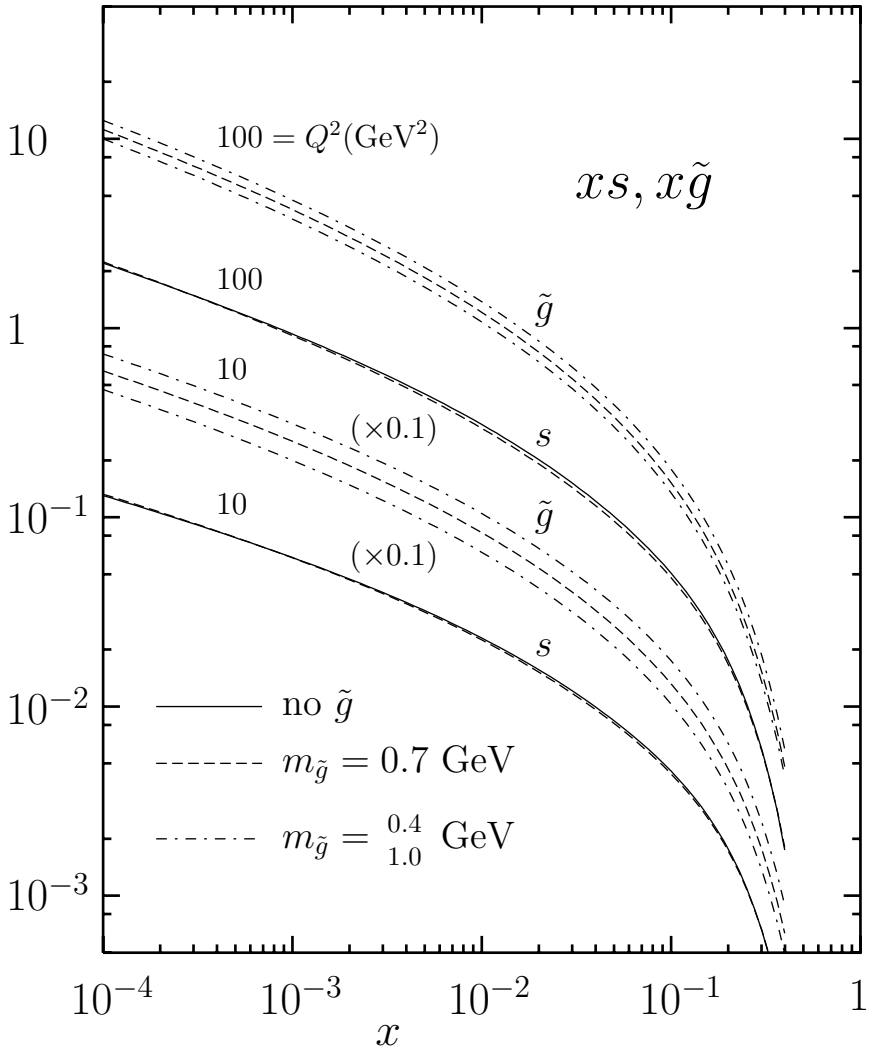

Figure 8: The radiatively generated NLO strange quark and gluino distributions of the proton. The gluino effects on xs are shown for a fixed gluino mass, while $x\tilde{g}$ is given for varying gluino masses.

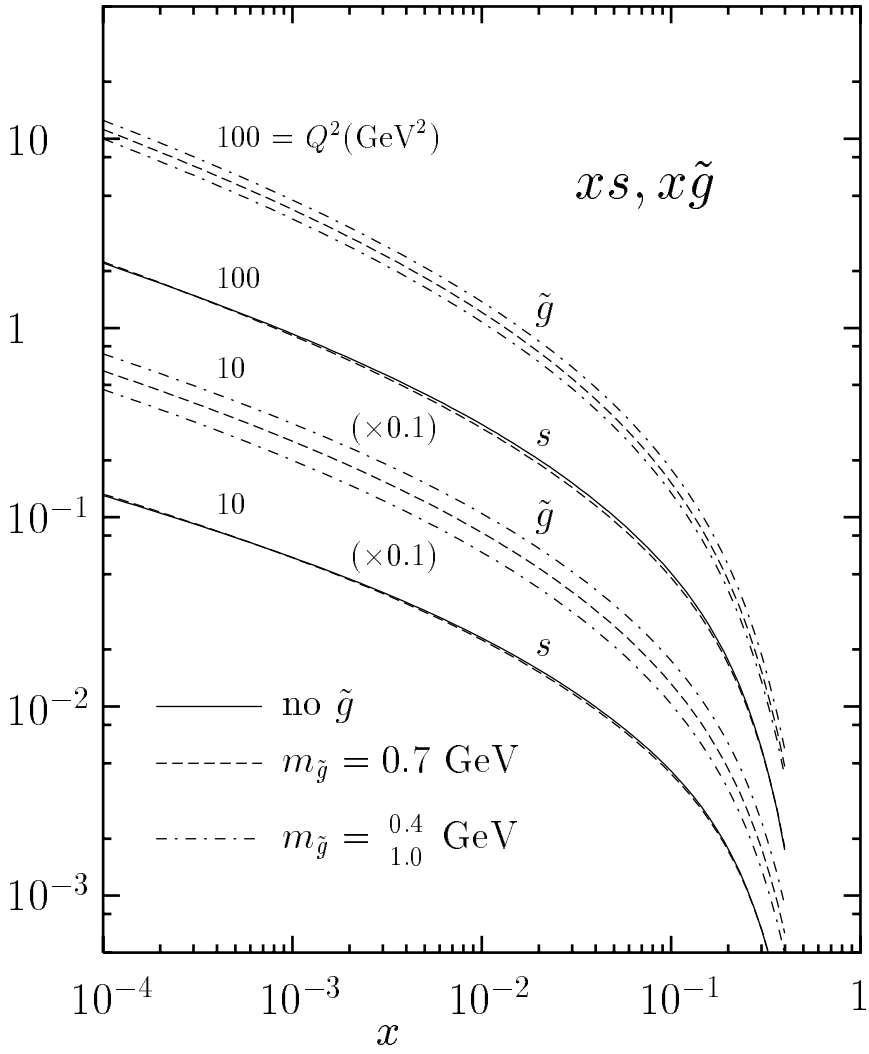

Figure 8: The radiatively generated NLO strange quark and gluino distributions of the proton. The gluino effects on xs are shown for a fixed gluino mass, while $x\tilde{g}$ is given for varying gluino masses.